

# Modelling and Analysis of Morphing Wing Structure for Variable Camber

Prathik Jain S<sup>1,\*</sup>, Sundarmahalingham A<sup>2</sup>, Sudhagara Rajan S<sup>3</sup>, Abhishek J<sup>4</sup>, Harshith G Hagalwadi<sup>5</sup>, Sanath S<sup>6</sup>, Tejas S M<sup>7</sup>

## Abstract

*This study explores the modelling and analysis of a morphing wing with variable camber configurations to observe its aerodynamic characteristics compared to conventional form. The morphing wing is the concept where the shape of the wing is altered mid-flight based on different phases of flight to improve its aerodynamic characteristics. Morphing wing structure designs such as the corrugated and FISHBAC designs were considered for this analysis. The NACA 2412 airfoil was selected among NACA 0012 and Wortmann 63-137 as it was suitable to accommodate the morphing actuation system and has better aerodynamic performance. In order to imitate the morphing wing movement, multiple models of morphing wing airfoils were modelled based on the deflections at the trailing edge using analytical calculations. These models were then used for aerodynamic analysis under similar conditions. The aerodynamic analysis showed the morphing structures better lift and lower drag at higher angles of attacks. They also had a delay in stall compared to the conventional airfoil. The wing design was modelled using CATIA V5, and static structural analysis was conducted in ANSYS to observe deformation under actuation loads. The study also evaluated three materials-Carbon Fiber Reinforced Polymer (CFRP), Polylactic Acid (PLA) and Acrylonitrile Butadiene Styrene (ABS)-to identify the suitable material for morphing wing applications. The analysis results showed ABS as the most suitable material due to its better deformation characteristics, making it ideal for achieving the desired deflection with less application of load. While CFRP demonstrated high stiffness, its minimal flexibility limited its effectiveness for actuation of the structure*

**Keywords:** Morphing wings, computational fluid dynamics, ABS, CFRP, PLA.

### \*Author for Correspondence

Prathik Jain S

<sup>1</sup>Associate Professor, Department of Aeronautical Engineering, Dayananda Sagar College of Engineering, Bengaluru, Karnataka, India

<sup>2</sup>Assistant Professor, Department of Aeronautical Engineering, Dayananda Sagar College of Engineering, Bengaluru, Karnataka, India

<sup>3</sup>Associate Professor, Department of Aerospace Engineering, School of Mechanical Engineering, REVA University, Bengaluru, Karnataka, India

<sup>4,5,6,7</sup>UG Student, Department of Aeronautical Engineering, Dayananda Sagar College of Engineering, Bengaluru, Karnataka, India

Received Date: January 22, 2025

Accepted Date: May 06, 2025

Published Date: May 23, 2025

**Citation:** Prathik Jain S, Sundarmahalingham A, Sudhagara Rajan S, Abhishek J, Harshith G Hagalwadi, Sanath S, Tejas S M. Modelling and Analysis of Morphing Wing Structure for Variable Camber. Journal of Polymer & Composites. 2025; 13(Special Issue 4): S209–S224p.

## INTRODUCTION

The concept of morphing wings is inspired from birds' natural ability to adjust their wing posture during flight. This approach has made way for improving aerodynamic efficiency, adaptability, and lower drag. The morphing wing concept was started from the Wright brothers' wing-warping technique, where the wings of the aircraft were bent and deflected to change the aerodynamic properties and fly. Further, the concept of morphing wings are developed through projects like NASA's Active Aeroelastic Wing etc.

The morphing wing concept involves dynamically changing the wing's geometry to improve aerodynamic performance at different phases of flight. This offers several benefits, including reduced drag, an improved lift-to-drag

ratio, and better endurance, range, and climb performance. The design integrates internal actuation mechanisms to enable smooth and continuous deformations while maintaining structural integrity.

Recent advancements in morphing have included use of special materials as Shape Memory Alloys, elastomeric skins, and carbon-Fiber composites for advanced actuation system. These improvements have made them lightweight, durable, and highly responsive morphing wing structures. Studies continue to show the potential of morphing wings in improving performance and efficiency. Yang et al. [1] demonstrated improved aerodynamic performance through morphing wing structure, while Cevdet Ozel et.al [2] explains the Morphing wing technology improves Unmanned Aerial Vehicle (UAV) efficiency, increasing payload and increase range, Scopelliti et al. [3] focused on chord wise bending with elastomeric skins, and Urban Fasel et al. [4], emphasized on the use of Continuous Carbon Fiber composite additive for morphing wing structures. Zi Kan et al. [5] describes the aerodynamic benefits of compliant leading-edge deflections in delaying stall than conventional flaps and improving different flight phases. Shivani Shankar et al. [6] conducted fatigue analysis on wing structures using different materials and spar across the cross-sections. Their study highlighted the role of material properties and structural design in improving wing strength and resistance to fatigue, relevant to morphing wing applications. C. Wang et.al [7] integrated a spiral pulley negative stiffness mechanism into the FishBAC morphing wing structure. James J. Joo et al. [8] introduced a variable camber compliant wing, enabling different camber modifications and enhancing aerodynamic performance through innovative mechanisms. Prathik S. Jain et al. [9] analysed one-way Fluid-Structure Interaction (FSI) to study flexible wing behaviour, highlighting its role in lightweight wing design and its relevance to morphing wing structure. Benjamin K. S. Woods et al. [10] compared computational methods like XFOIL and OpenFOAM for analysing active camber morphing, validating their capability to model aerodynamic performance and compare. Tomohiro Yokozeki et al. [11] integrated corrugated composite structures into morphing airfoils, showing better lift and control through wind tunnel testing at high speeds. Iman Dayyani et al. [12] developed elastomer-coated composite skins optimized for morphing applications, achieving improved stiffness and reduced power requirements for actuation. Koray Özsoy [13] compares the materials like Acrylonitrile butadiene Styrene (ABS) and Poly Lactic Acid (PLA) based on their mechanical properties. It finds that PLA generally exhibits higher tensile and compressive strength than ABS, with mechanical properties highly depending on fill density of the structure. Sudhir Jain Prathik et al. [14] discusses about the developing of airship shapes for better aerodynamic efficiency at different flight conditions. M.S.H. Al-Furjan [15] reviewed the mechanical properties of CFRP and Kevlar composites, highlighting their applications in various fields like civil, aerospace, and military industries. K.K. Herbert Yeung [16] studies on the Kevlar-49 fiber-reinforced thermoplastic composites material properties, highlighting their high tensile strength and modulus, and compares them with traditional glass and Carbon Fiber Reinforced Composites (CFRP). Pecora R [17] developed a multimodal camber morphing wing flap for large civil aircraft under the Clean Sky program, using finger-like robotic ribs driven by electromechanical actuators. Moens F [18] investigated morphing technology for a turboprop regional aircraft wing under the Clean Sky 2 AIRGREEN2 program, focusing on a deformable droop nose and a multi-functional segmented flap. de Gaspari A et al. [19] designed a leading-edge morphing system based on compliant structures for a twin-prop regional aircraft to enhance aerodynamic efficiency. Mamou M et al. [20] optimized aerodynamic performance of a wind tunnel morphing wing using smart material actuators to enhance laminar flow and reduce drag. The paper proposes a modular structure for smooth shape changes and the other by validating a control system that optimizes the wing's shape for better aerodynamic efficiency. [21,22]. Manoranjan Majji et al focused on modular designs for smooth deformation, control systems for real-time shape optimization, and twist-based designs to enhance aerodynamic performance and delay stall [23]. Veenstra [24] paper outlines the random vibration analysis of a structural wing model designed for an electric Vertical Takeoff and Landing (VTOL) UAV called the Manta.

## MATERIALS AND METHODS

The project methodology starts with reviewing different morphing wing design concepts developed by others and selection of few design concepts. Additionally, several airfoils were compared to select the airfoil with better aerodynamic characteristics and accommodates the morphing structure.

### Selection of Air foil

The airfoil were plotted using XFLR5 software. Where, based on the studies the Reynolds number is set at 250000 and 15m/s as the velocity at which the air is flowing. Using Equation (1).

$$Re = \frac{\rho v l}{\mu} = \frac{\rho v l}{\nu} \quad (1)$$

From the study, three airfoils—NACA 0012, NACA 2412, and Wortmann 63-137, were considered for aerodynamic analysis. The Co-ordinates of these airfoils were obtained from the aerofoil tools database. The analysis was performed using XFLR5 to evaluate their aerodynamic characteristics. The Coefficient of lift ( $C_l$ ) versus angle of attack of the airfoil ( $\alpha$ ) curves were generated to assess the performance of each airfoil. The plots of  $C_l$  vs  $\alpha$  and  $C_l/C_d$  vs  $\alpha$  for different airfoils is plotted in the Figure 1 (a) and (b).

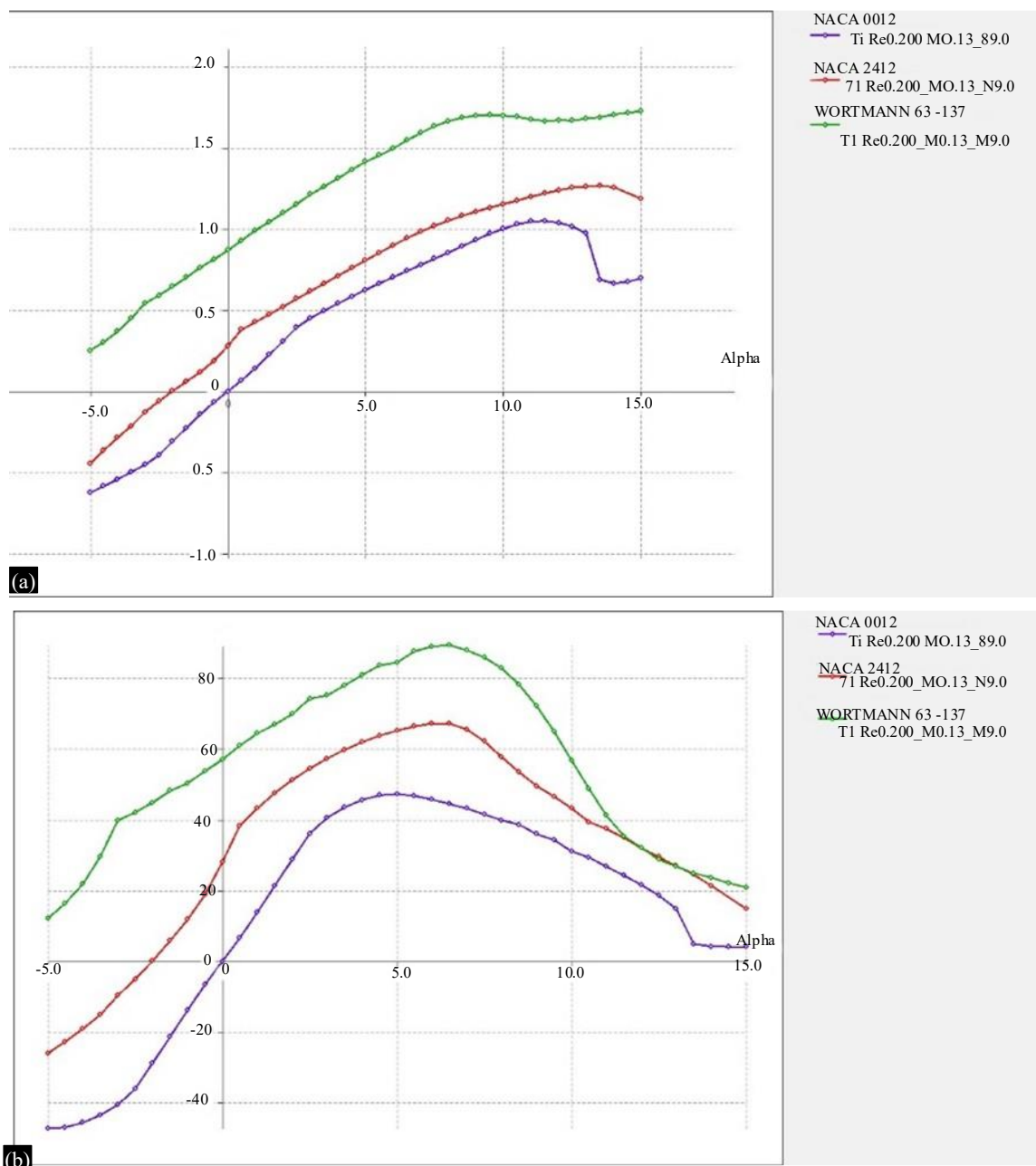


**Figure 1.** (a)  $C_l$  vs  $\alpha$  (b)  $C_l/C_d$  vs  $\alpha$ .

For better understanding and easier comparison, a Pugh matrix was used to compare the results of NACA 0012, NACA 2412, and Wortmann 63-137 airfoil based on fabrication,  $C_{l_{max}}$ ,  $C_l/C_d$  and stall angle. NACA 2412 was chosen for its higher stall angle, smoother stall characteristics, lower drag at moderate angles, better lift-to-drag ratio, and better pitch stability, making it the most efficient and stable option for the design. The Airfoils are evaluated on the basis of a grading scale where grades are given on how well they meet the requirements, here 5 is the maximum grade given and 1 is the lowest grade given. This is summarized in Table 1.

### Material Selection

Three different materials, which includes composite and polymer categories, were selected to compare their deformation behaviors under similar loading conditions. The properties of these materials are shown in Table 2.

### Generation of 3D Model

The coordinates of the airfoil were imported into modelling software, where the airfoil is extended to a length of 20mm and a rectangular spar is constructed. The chord, measuring 800mm, represents the length between the leading and trailing edge of the wing. Figure 2 (a) shows the image of the FISHBAC Structure and Figure 2 (b) shows the Corrugated Structure.

### Morphing Wing Geometry

In order to understand the Aerodynamic properties of the morphing airfoil, the changed geometry of the airfoil when they are deflected must be modeled for ease of analysis. To achieve this, the airfoil baseline is modified by introducing chamber to specific sections of the chord. As shown in Figure 3, the leading edge is fixed and does not undergo morphing. The point where the morphing begins is defined by the parameter  $x_s$ , which is the key variable of this report. The airfoil's is generated by applying the thickness distribution onto the calculated camber line. Just like the standard NACA airfoils, the thickness is added perpendicular to the camber line at every point of the airfoil.

**Table 1.** Pugh Matrix.

Parameters	NACA 0012	NACA 2412	Wortmann 63-137
$C_{l_{max}}$	3	4	5
$\alpha_{Stall}$	4	5	3
$C_l/C_d$	3	4	4
Total	10	13	12

**Table 2.** Properties of different materials.

Material	Polylactic acid (PLA)	Acrylonitrile butadiene styrene (ABS)	Carbon fiber reinforced polymer (CFRP)
Density(kg/m <sup>3</sup> )	1260	1050	1600
Young's Modulus(MPa)	2454	2300	150000
Poisson's ratio	0.33	0.35	0.3

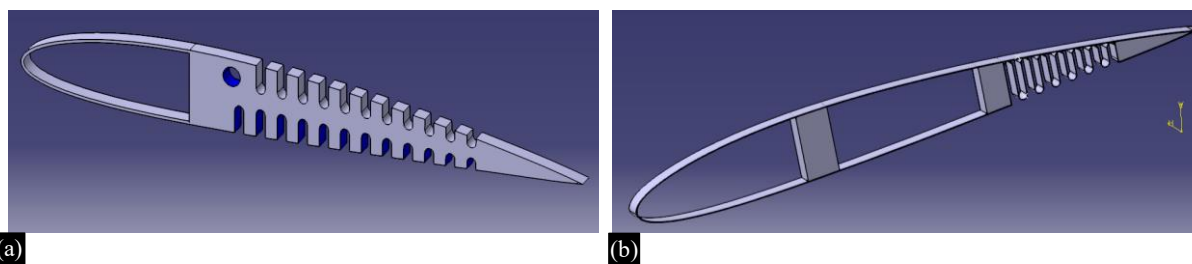


**Figure 2.** (a) FISHBAC Structure (b) Corrugated structure.

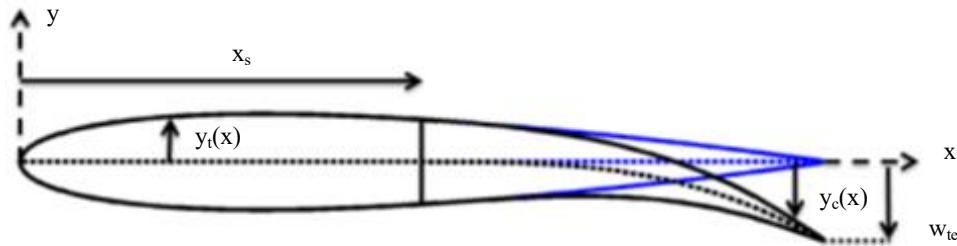


**Figure 3.** Morphing wing geometry definition [10].

The non-dimensional thickness distribution,  $y_t(x)$  for NACA airfoils with 4 series, is defined by,

$$y_t(x) = \frac{t}{0.2} [0.2969\sqrt{x} - 0.1260x - 0.3516(x)^2 + 0.2843(x)^3 - 0.1015(x)^4] \quad (2)$$

Where,

$x$  is the chord length (non-dimensional)

$t$  is the airfoil thickness (non-dimensional) ( $t = 0.12$  for a NACA 2412)

3<sup>rd</sup> order polynomial shape function is used to represent the morphing wing chamber line This is particularly effective for modeling morphing camber designs that depend on the bending or flexibility of internal structural elements. In this study, the function is specifically designed to allow precise control over how much the trailing edge deflects.

$$y_c = \begin{cases} 0, & 0 \leq x \leq x_s \\ \frac{-w_{te}}{(1-x_s)^2} (x - x_s)^3, & x_s \leq x \leq 1 \end{cases} \quad (3)$$

Where,

$w_{te}$ - Maximum trailing edge deflection of the camber line (non-dimensional)

The values thickness distribution ( $y_t$ ) across the airfoil is overlaid perpendicularly on the camber deflection,  $y_c$ , to get the coordinates for the upper ( $x_u, y_u$ ) and lower ( $x_l, y_l$ ) surfaces, according to,

$$x_u = x - y_t \sin \theta \quad (4)$$

$$x_l = x + y_t \sin \theta \quad (5)$$

$$y_u = y_c + y_t \cos \theta \quad (6)$$

$$y_l = y_c - y_t \cos \theta \quad (7)$$

Where ,

the local slope of the camber line ( $\theta$ ) , calculated using,

$$\theta(x) = \tan^{-1} \left( \frac{dy_c}{dx} \right) \quad (8)$$

This simple approach to defining the shape of an active camber morphing airfoil makes it easy to quickly and efficiently explore a wide variety of configurations.

Based on the calculations, The Figure 4 (a) shows the morphing airfoil plotted for 0.05 deflection (i.e., for 800mm chord, it will be 40mm deflection) and Figure.4 (b) shows the morphing airfoil plotted for 0.1 deflection (i.e., for 800mm chord, it will be 80mm deflection).



**Figure 4.** (a) & (b) Morphing wing geometry's.

### Computational Fluid Dynamics Analysis

The CFD analysis was conducted to determine the aerodynamic properties of the morphing wing across various angles of attack ( $\alpha$ ). The study used numerical simulations using tools like ANSYS Fluent to evaluate the lift and drag coefficients NACA 2412 and morphing models. Simulations were carried out under specified Reynolds number, approximating 2,500,000, to imitate the required conditions. The analysis highlighted how the morphing wing's geometry adapts to optimize aerodynamic performance, particularly by reducing drag and increasing lift-to-drag ratios during different phases. The results were plotted and used for further comparisons.

### Static Structural Analysis

Static analysis was performed to study the structural integrity and deformation behaviour of the morphing wing under varying aerodynamic loads. FEA was conducted using ANSYS to determine stress distributions and displacement across the wing structure. The study was conducted on the selected morphing mechanisms, FISHBAC and corrugated structures. The analysis was done to determine the design which require minimal actuation load to attain required deflection, which would reduce the need of more powerful and heavier actuation system. This balance between strength and adaptability is crucial for the wing's performance across different flight conditions. Additionally, selection of appropriate material id also necessary for the structural strength and ease in adapting to different conditions.

## RESULTS

### Structural Analysis Results

The static structural analysis provides the structural properties and nature of the both designs and its responsiveness upon application of loads. In this analysis, the leading edge of the structure is fixed, while a force is applied at the trailing edge to measure the resulting deflection. Multiple iterations with varying force values were conducted on both designs to identify the force required to achieve the desired deflection found from the aerodynamic analysis. After several iterations, it was determined that a minimum applied force of approximately 4 N was needed to achieve desired deflection. This force value

will be utilized as the reference load for further analysis. The total deformation results from the static analysis for both structures are presented in Table 3 and Figure 5 (a) & (b) illustrates the deflection characteristics of both structures.

From the above results, the corrugated structure showed the highest deformation, which is similar to the value of the deflection of the morphing wing from the aerodynamic analysis. This concludes that the corrugated structure requires least amount of the actuation force to perform the required deflection at the trailing edge. This reduces the need for stronger actuation system which would require more space. Additionally, in order to determine which material would be better for morphing wing, a material analysis was conducted between ABS, PLA and CFRP materials. All the materials properties were applied to the corrugated structure design and analysis were conducted under similar conditions. The Structural Analysis of the materials determines the deformation, Von Misus Stress etc. Additionally, Fatigue Analysis was also conducted to determine the fatigue nature of these materials on the design. The Table 4 represents the structural and fatigue analysis of the ABS to accommodate and increase the overall weight.

**Table 3.** Total Deflection of morphing Structure.

Structure	Total deflection (in mm)	
FISHBAC	Minimum	0
	Maximum	12.27
Corrugated	Minimum	0
	Maximum	76.147

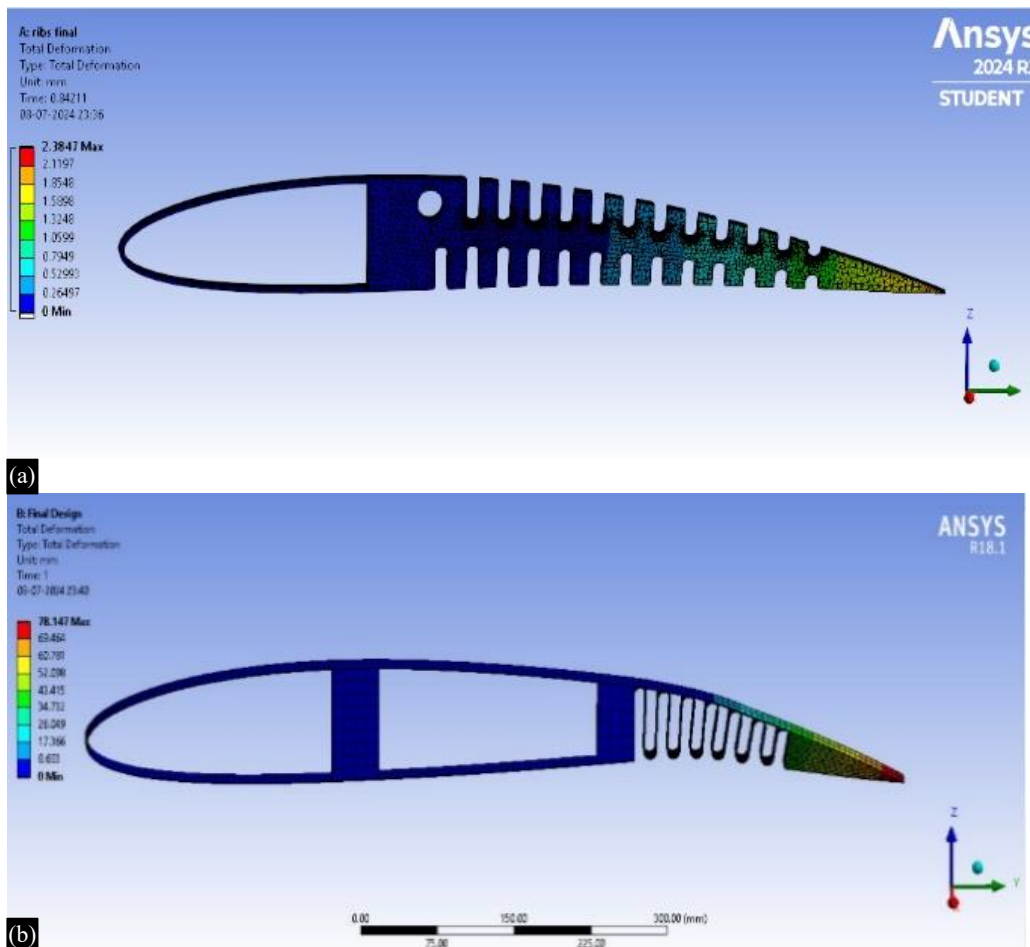


**Figure 5.** Total deflection (a) FISHBAC structure (b) corrugated structure.

**Table 4.** Structural and Fatigue analysis for ABS material.

Property	Value
Von Misus Stress (MPa)	151.91
Total Deformation (mm)	90.285
Shear Stress (MPa)	87.36
Fatigue Life (Cycles)	1 x 10 <sup>7</sup>
Max Equivalent Stress (MPa)	151.91

**Table 5.** Structural and Fatigue analysis for PLA material.

Property	Value
Von Misus Stress (MPa)	126.25
Total Deformation (mm)	76.147
Shear Stress (MPa)	70.84
Fatigue Life (Cycles)	5.5 x 10 <sup>7</sup>
Max Equivalent Stress (MPa)	122.32

**Table 6.** Structural and Fatigue analysis for CFRP material.

Property	Value
Von Misus Stress (MPa)	50.13
Total Deformation (mm)	3.34
Shear Stress (MPa)	26.54
Fatigue Life (Cycles)	>10 <sup>7</sup>
Max Equivalent Stress (MPa)	151.91

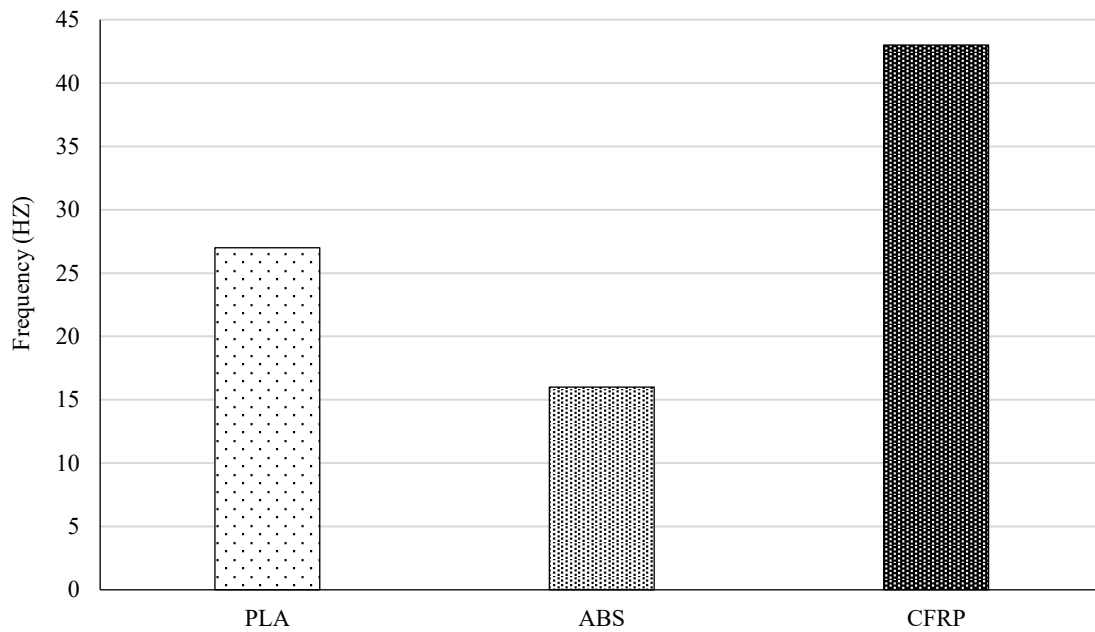
Similarly Table 5 and 6 represents the structural and Fatigue analysis results of PLA and CFRP materials respectively.

Based on the analysis, ABS and PLA exhibit significantly higher maximum deformations (90.285 mm and 76.147 mm, respectively) compared to CFRP (1.6742 mm). This makes ABS and PLA more suitable candidates for morphing wing applications due to their ability to deform more substantially under similar conditions. Although PLA offers better fatigue resistance than ABS, it is stiffer and requires more actuation power, making it less efficient for continuous morphing applications. CFRP, despite its exceptional strength and fatigue life, is highly stiff and requires significant actuation power, making it impractical for morphing applications. CFRP may not be ideal for morphing due to its rigidity, it could still be useful for supporting structural components where minimal deformation is required. Therefore, ABS corrugated structures provide the best balance of flexibility, durability, low weight, and cost-effectiveness, making them the optimal choice for morphing UAV wings where adaptability and lightweight design are crucial for performance.

### Vibrational Analysis

The vibrational analysis was conducted in ANSYS for the corrugated structure using PLA, ABS, and CFRP Materials. The vibration simulates conditions where the structure is exposed to a spectrum of frequencies rather than a single harmonic input. A Power Spectral Density (PSD) profile was applied in the Z-direction to mimic such an environment. Modal analysis was first conducted to identify the structure's natural frequencies and mode shapes, followed by a vibration analysis.

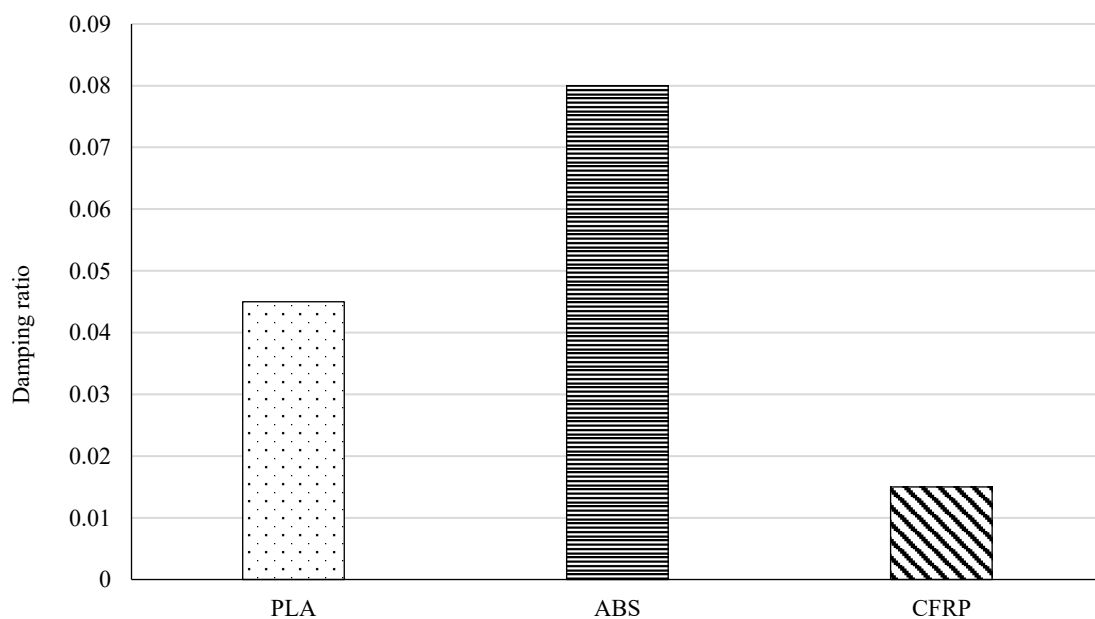
Figure 6 illustrates the natural frequencies of the three materials, providing insight into their relative stiffness. CFRP exhibits the highest natural frequency at 42.18 Hz, indicating it is the most rigid and resistant to bending. On the other hand, ABS has the lowest frequency at 16.65 Hz, making it the most flexible and prone to movement during vibration. PLA is moderately stiff, with a natural frequency of 25.4 Hz.



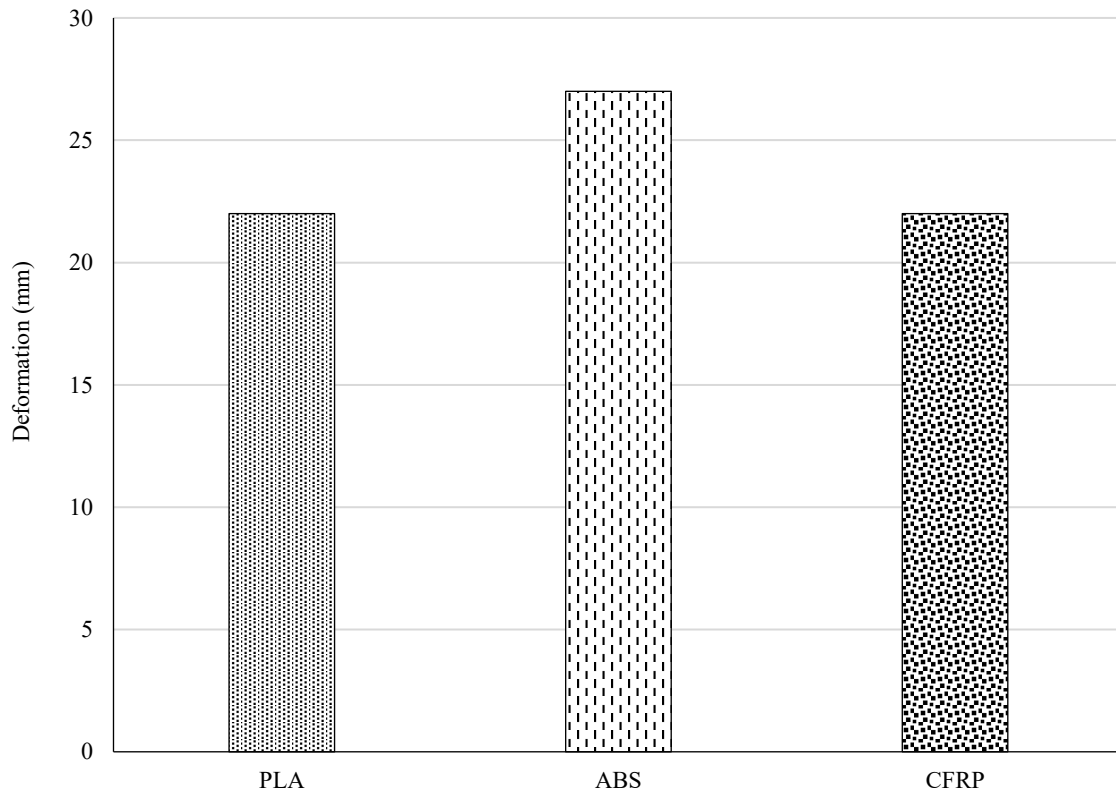
**Figure 6.** Natural Frequency of all materials.

Figure 7 presents the vibration damping performance of each material. ABS demonstrates the highest damping ratio at 0.08, indicating strong capability in absorbing vibrations and reducing oscillations swiftly. PLA shows a moderate damping ratio of 0.045. In contrast, CFRP has the lowest damping ratio at 0.012, suggesting it is less effective at damping and allows more vibration to pass through.

Figure 8 illustrates the deformation behavior of different materials under vibrational loading. Among the materials tested, ABS exhibits the highest deformation at 28.19 mm, indicating its ability to absorb vibrational energy through greater flexibility. PLA shows moderate deformation of 22.85 mm whereas, CFRP demonstrates the least deformation at 20.3 mm, due to its high stiffness and resistance to vibrational deflection.



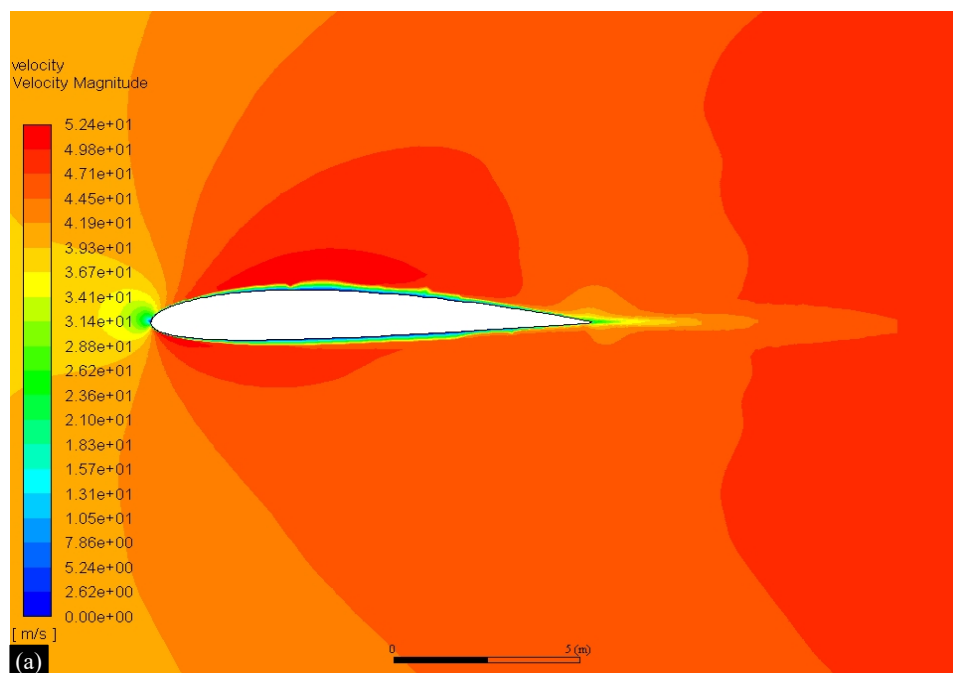
**Figure 7.** Damping Ratio of all materials.

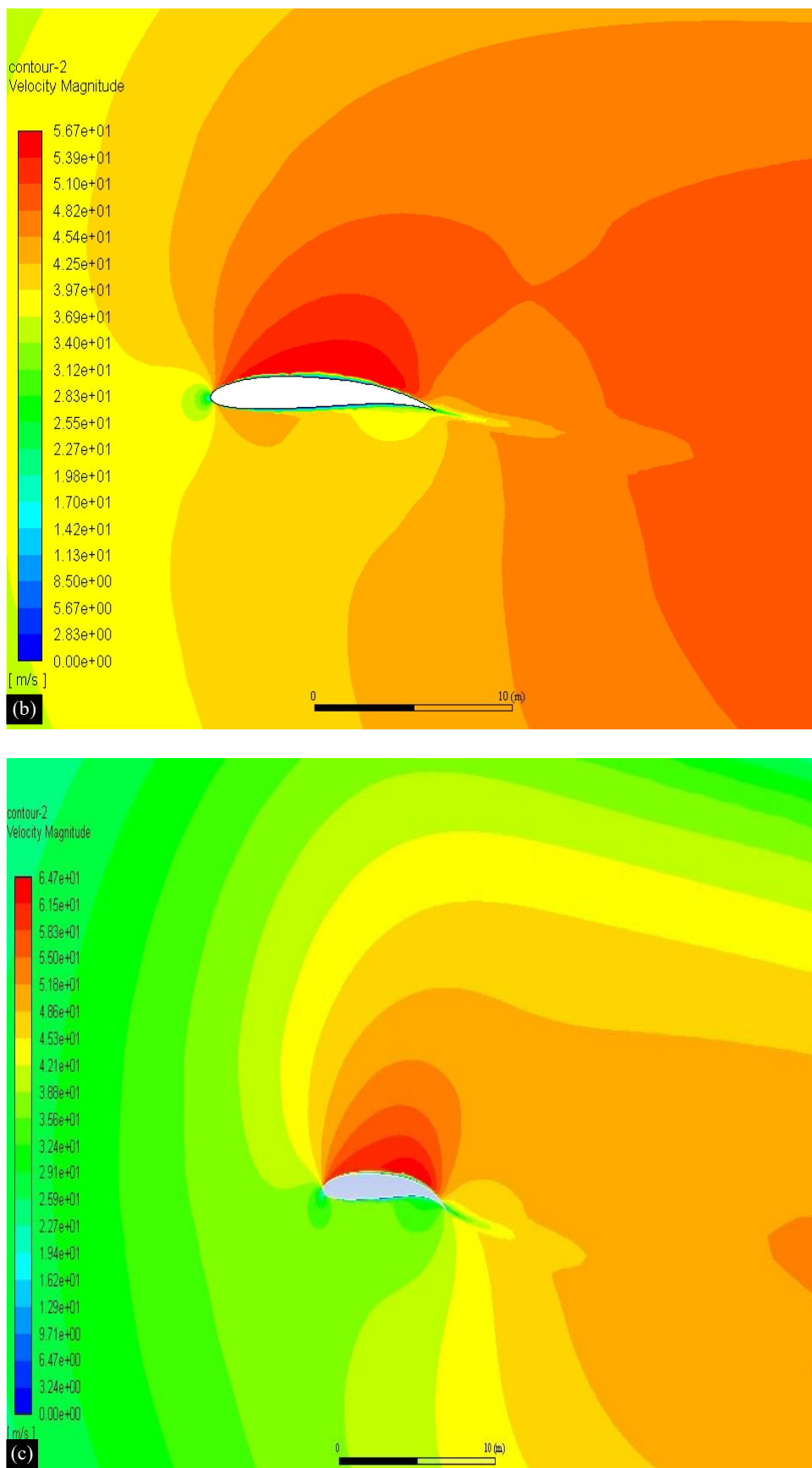


**Figure 8.** Deformation of different materials at a particular vibration.

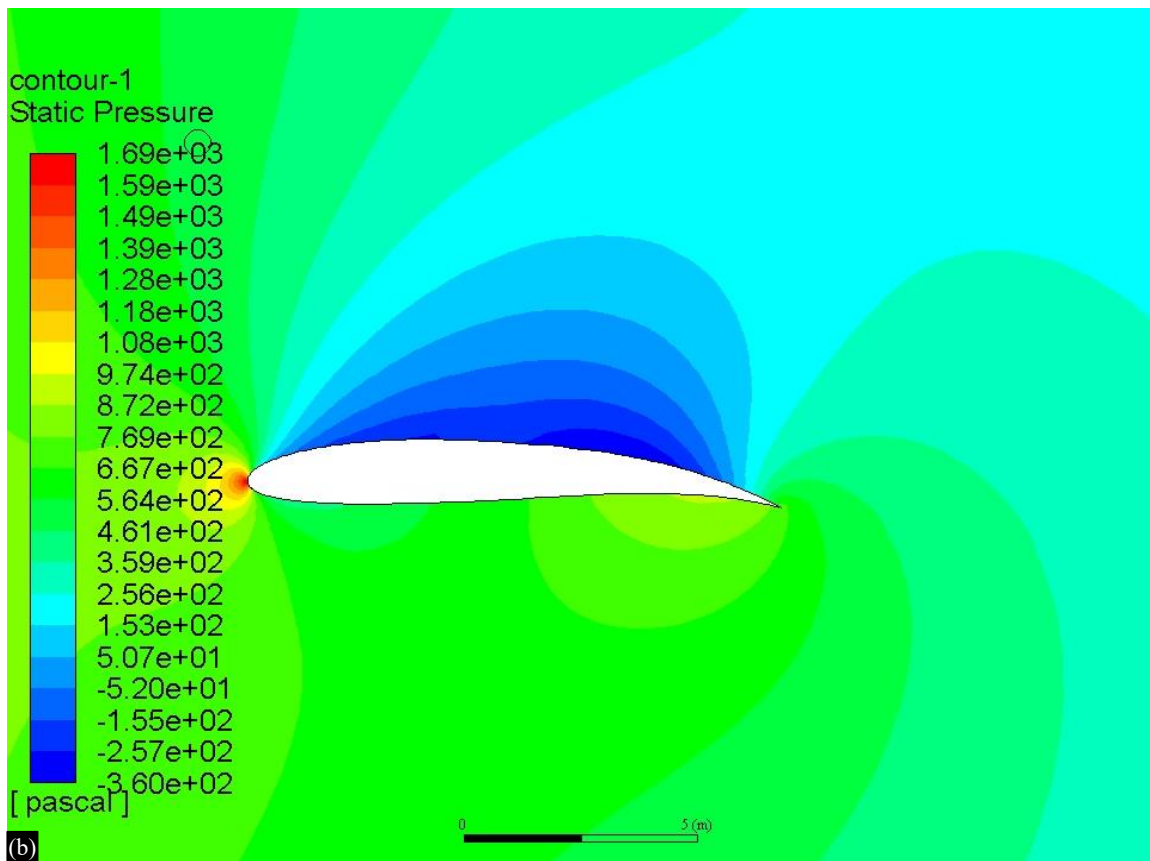
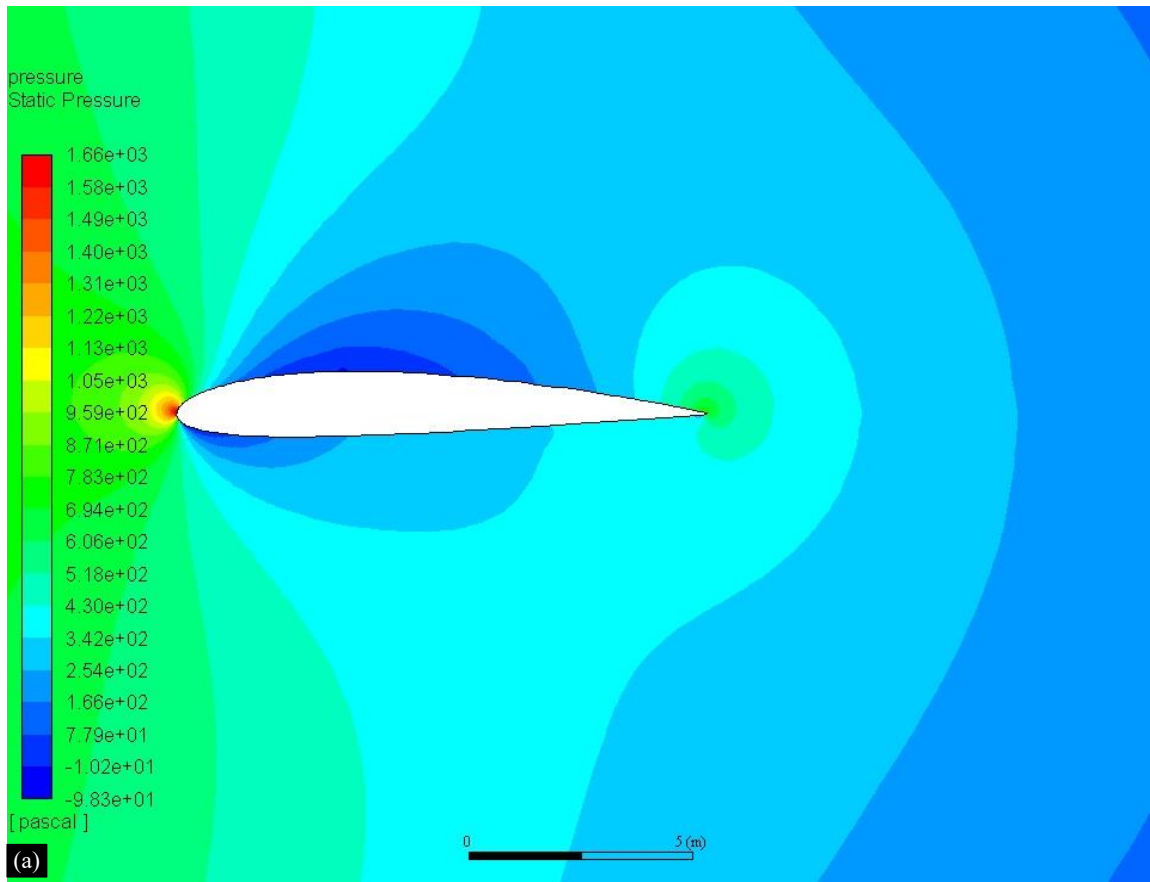
**Aerodynamic Characteristics**

In order to see the variation in the aerodynamic properties, the CFD analysis is conducted to calculate the values of lift and drag for different  $\alpha$  for various models of morphing models. The analysis provided the velocities and pressure contours of the 3 models at various angle of attack. The Figure 9 and Figure 10 represents the Velocity and Pressure contours of the 3 models at  $0^\circ$  Angle of Attack.





**Figure 9.** Velocity contours (a. 0 Deflection, b. -40mm Deflection, c. -80 mm Deflection).



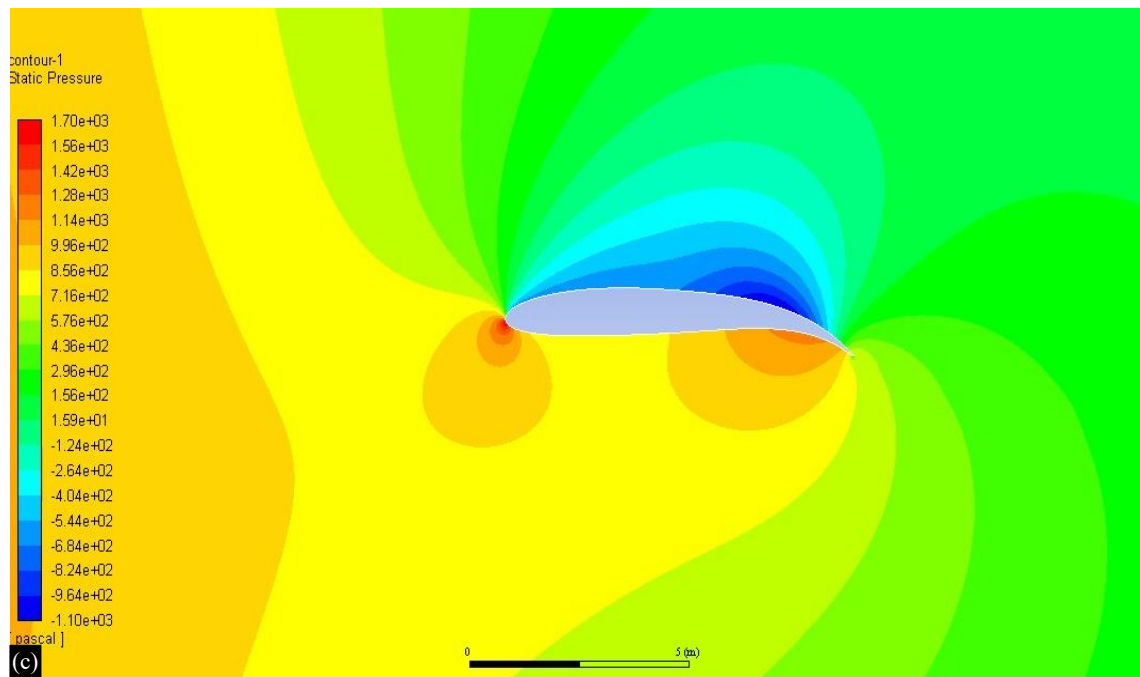


**Figure 10.** Pressure contours, (a) 0 Deflection, (b) -40 mm Deflection, (c) -80 mm Deflection

From the plot of lift versus  $\alpha$  Figure 11, it can be observed that with the increase in the  $\alpha$  the lift gradually increases until it reaches a maximum at the stall angle. After this point, any further increase in  $\alpha$  reduces the lift. It was observed that the airfoils with deflection had higher lift Vs  $\alpha$  curves compared to the conventional airfoil. The lift increased with the deflection of the airfoil.

The plot for drag versus  $\alpha$  is given below in the Figure 12, from the plot it can be observed that the drag increases with the increase in the  $\alpha$ . The drag increase with the deflection due to increase in lift and due to skin friction. The conventional airfoil has the least drag compared to others.

The plot between  $C_l/C_d$  Vs  $\alpha$  Fig. 13, shows the variation of the Aerodynamic efficiency with change in  $\alpha$ . This demonstrates that while deflection improves control and lift at lower speeds, it generally decreases the overall aerodynamic efficiency ( $C_l/C_d$  ratio) and shifts the peak performance to lower  $\alpha$ .

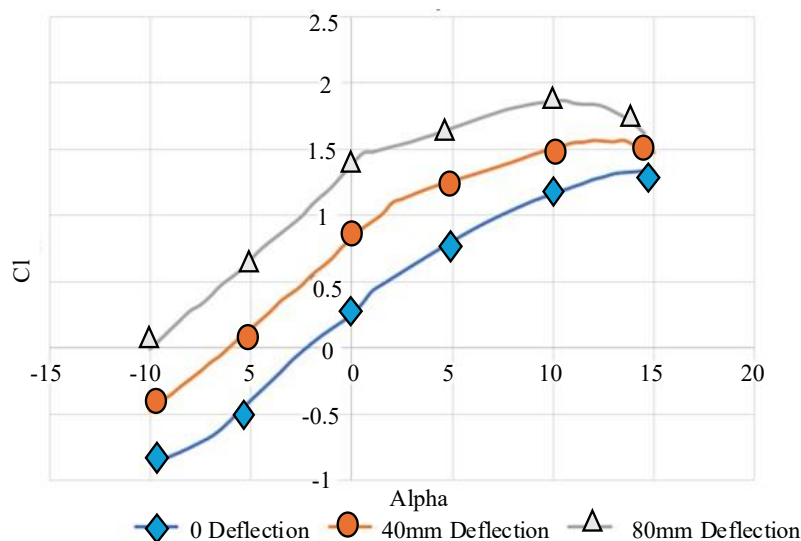


**Figure 11.**  $C_l$  Vs  $\alpha$ .

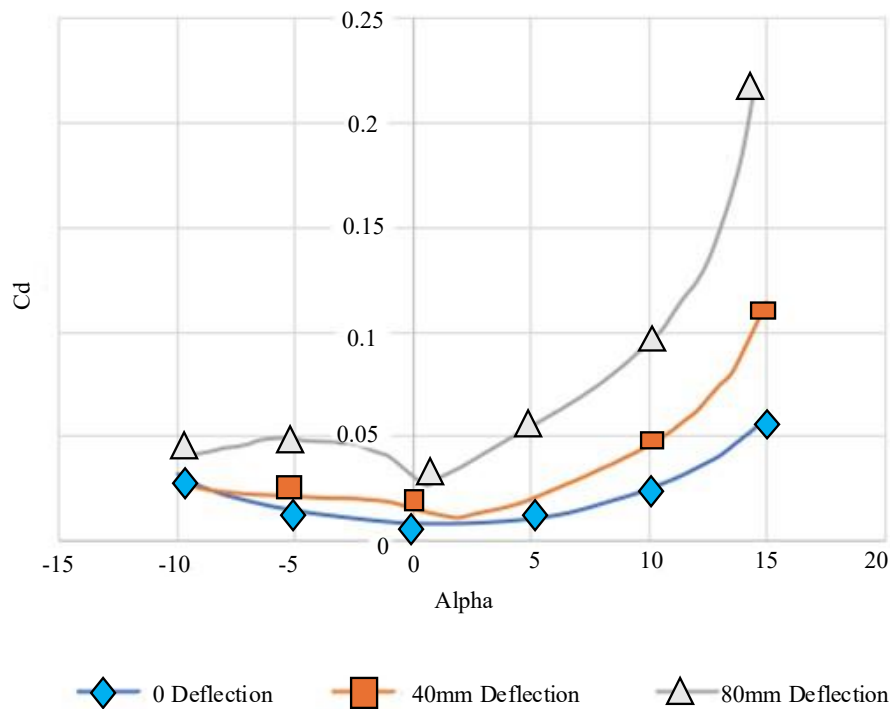


Figure 12.  $C_d$  Vs  $\alpha$ .

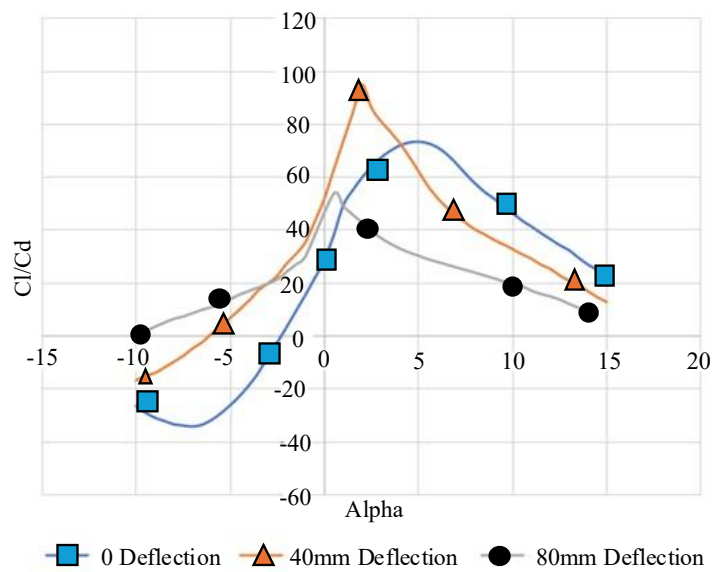


Figure 13.  $C_l/C_d$  Vs  $\alpha$ .

### CONCLUSION

The aerodynamic performance of NACA 0012, NACA 2412, and Wortmann 63-137 airfoils was initially evaluated using XFLR5 software. Among these, NACA 2412 exhibited the most favorable aerodynamic characteristics. Based on these findings, wing models incorporating both FISHBAC and corrugated structures were developed using CATIA V5. Subsequent static structural analysis showed that the corrugated design experienced higher deformation under comparatively lower stress, suggesting increased flexibility. CFD simulations demonstrated that morphing wing configurations offer enhanced aerodynamic efficiency over traditional wing designs. These designs showed significant improvements in lift generation, control, and airflow characteristics across a range of angles of attack. The morphing capability allowed the wings to adapt dynamically to varying flight conditions, resulting in improved

lift-to-drag ratios and delayed onset of stall, thereby validating the aerodynamic benefits of adaptable wing structures. Additionally, this adaptability was achieved with relatively low actuation force, enhancing the feasibility of practical morphing mechanisms. Materials including ABS, PLA, and CFRP were evaluated for their suitability in wing fabrication. Among this ABS was chosen due to its higher deformation tolerance, reasonable stress handling, and strong fatigue resistance. Vibrational analysis further revealed that ABS possessed superior damping properties, which are critical for minimizing structural vibrations and maintaining flight stability. Overall, the integration of a corrugated morphing wing structure using ABS material emerges as a promising approach for UAVs and similar applications, where lightweight construction, aerodynamic adaptability, and structural responsiveness are essential.

### Acknowledgements

We sincerely express our gratitude to Dayananda Sagar College of Engineering for providing the invaluable support and facilities that played a crucial role in the successful completion of our project.

### REFERENCES

1. Yang H, Jiang S, Wang Y, et al. Design, kinematic and fluid-structure interaction analysis of a morphing wing. *Aerospace Science and Technology*. 2023;143:108721p. doi:10.1016/j.ast.2023.108721.
2. Ozel C, Ozbek E, Ekici S. A review on applications and effects of morphing wing technology on UAVs. *International Journal of Aviation Science and Technology*. 2020; 1(01): 30-10p. doi: 10.23890/IJAST.vm01is01.0105.
3. Martinez JM, Scopelliti D, Bil C, et al. Design, analysis and experimental testing of a morphing wing. *Proceedings of the 25th AIAA/AHS Adaptive Structures Conference*; 2017 Jan 9-13; Grapevine, Texas, USA: AIAA SciTech Forum; 2017. 1-8p.
4. Fasel U, Keidel D, Baumann LC, et al. Composite additive manufacturing of morphing aerospace structures. *Manufacturing Letters*. 2020; 23: 85-8p. doi: 10.1016/j.mfglet.2019.12.004.
5. Zi KAN, Daochun LI, Tong SHEN, et al. Aerodynamic characteristics of a morphing wing with flexible leading-edge. *Chinese Journal of Aeronautics*. 2020; 33(10):2610-9p. doi: 10.1016/j.cja.2020.03.012
6. Shankar S, Jain PS, Chandru V, et al. Fatigue analysis on wing structure. *AIP Conf. Proc*; 2021; 2317(1), 040013. doi: 10.1063/5.0036270
7. Wang C, Zhang J, Shaw A, et al. Integration of the spiral pulley negative stiffness mechanism into the FishBAC morphing wing. In: Benjeddou A, Mechbal N, Deu J.F., (Eds.) *9th ECCOMAS Themat. Conf. Smart Struct. Mater*; 2019 Paris, France.
8. Joo JJ, Marks CR, Zientarski L, et al. Variable camber compliant wing-design. *Proceedings of 23rd AIAA/AHS Adaptive Structures Conference*; 2015 Jan 5-9; Kissimmee, FL, USA. Reston, VA: AIAA; 2015. doi: 10.2514/6.2015-1050
9. Prathik SJ, Kshiti PG, Shivani S, et al. Fluid-Structure Interaction Study of a Wing Structure. *International Research Journal of Engineering and Technology*. 2021; 8(05): 2516-27p.
10. Woods BK, Fincham JH, Friswell MI. Aerodynamic modeling of the fishbone active camber morphing concept. *Proceedings of the Applied Aerodynamics Conference*; 2014 July 22-24. Bristol, UK: Royal Aeronautical Society (RAeS); 2014.
11. Yokozeki T, Sugiura A, Hirano Y. Development of variable camber morphing airfoil using corrugated structure. *Journal of Aircraft*. 2014; 51(3): 1-7p. doi: 10.2514/1.C032573
12. Dayyani I, Woods BK, Friswell MI, et al. The optimal design of a coated corrugated skin for the FishBAC morphing wing. Paper presented at: *24th International Conference on Adaptive Structures and Technologies*. 2013 October 7-9.
13. Özsoy K, Erçetin A and Çevik ZA. Comparison of mechanical properties of PLA and ABS-based structures produced by fused deposition modeling additive manufacturing. *European Journal of Science and Technology*. 2021; 27: 802-9p. doi: 10.31590/ejosat.983317
14. Prathik JS, Sundaramahalingam A, Sudhagara Rajan S, et al. Innovative airship design for real-time air quality monitoring using IoT technology. *Journal of Applied Engineering Science*. 2024; 22(4): 727-38p. doi:10.5937/jaes0-51157

15. Al-Furjan MSH, Shan L, Shen X, et al. A review on fabrication techniques and tensile properties of glass, carbon, and Kevlar fiber reinforced Polymer composites. *Journal of Materials Research and Technology*. 2022; 19: 2930-59p. doi: 10.1016/j.jmrt.2022.06.008
16. Yeung KH, Rao KP. Mechanical properties of Kevlar-49 fiber reinforced thermoplastic composites. *Polymers and Polymer Composites*. 2012; 20(5): 411-24p. doi: 10.1177/096739111202000501
17. Pecora, R. Morphing wing flaps for large civil aircraft: Evolution of a smart technology across the Clean Sky program. *Chinese Journal of Aeronautics*. 2021; 34(7):13-28p. doi:10.1016/j.cja.2020.08.004.
18. Frédéric Moens. Augmented aircraft performance with the use of morphing technology for a turboprop regional aircraft wing. *Biomimetics*. 2019; 4(3):1-20p. doi:10.3390/biomimetics4030064.
19. de Gaspari A, Gilardelli A, Ricci S, et al. Design of a Leading Edge Morphing Based on Compliant Structures for a Twin-Prop Regional Aircraft. In *Proceedings of the AIAA/AHS Adaptive Structure Conference*; 2018 8-12 January. Kissimmee, FL, USA; 2018. doi:10.2514/6.2018-1063.
20. Mamou M, Mébarki Y, Khalid M, et al. Aerodynamic performance optimization of a wind tunnel morphing wing model subject to various cruise flow conditions. In *27th International Congress of the Aeronautical Sciences ICAS*. 2010 September; 1-25p.
21. Michel Joel Tchatchueng Kammegnea, Ruxandra Mihaela Boteza, et al. Proportional fuzzy feed-forward architecture control validation by wind tunnel tests of a morphing wing. *Chinese Journal of Aeronautics*. 2017; 30(2): 561-576p. doi:10.1016/j.cja.2017.02.001.
22. Rosario Pecora. Morphing wing flaps for large civil aircraft: Evolution of a smart technology across the Clean Sky program. *Chinese Journal of Aeronautics*. 2017; 34(7): 13-28p. doi:10.1016/j.cja.2020.08.004
23. Manoranjan Majji, Othon K. Rediniotis et al. Design of a Morphing Wing : Modeling and Experiments. In *Proceedings of AIAA Atmospheric Flight Mechanics Conference and Exhibit*; 2007 August, 6310p. doi: 10.2514/6.2007-6310.
24. Veenstra, Noah, and Joana Rocha. Vibration Analysis of an Electric UAV Wing Model. *Canadian Acoustics* ; 2022, Vol 50: No. 3: 70-1p.